Bioorganic & Medicinal Chemistry 19 (2011) 603–612

Contents lists available at ScienceDirect

Bioorganic & Medicinal Chemistry

journal homepage: www.elsevier.com/locate/bmc

Cytotoxicity and topoisomerase I/II inhibition of glycosylated 2-phenyl-indoles, 2-phenyl-benzo[*b*]thiophenes and 2-phenyl-benzo[*b*]furans

Wei Shi, Sandra L. Marcus, Todd L. Lowary *

Alberta Ingenuity Centre for Carbohydrate Science and Department of Chemistry, The University of Alberta, Gunning-Lemieux Chemistry Centre, Edmonton, AB T6G 2G2 Canada

ARTICLE INFO

Article history:
Received 5 July 2010
Revised 21 October 2010
Accepted 26 October 2010
Available online 30 October 2010

Keywords:
Anthracycline
Functional mimetics
Cytotoxicity
Topoisomerase inhibition

ABSTRACT

A panel of glycosylated DNA binding agents (**1**–**12**) designed as functional anthracycline mimics was screened against three solid-tumor cell lines (MCF-7, HT 29 and HepG2/C3A) and three non-tumor cell lines by the MTS (3-(4,5-dimethylthiazol-2-yl)-5-(3-carboxymethoxyphenyl)-2-(4-sulfophenyl)-2*H*-tetrazolium) cell viability assay. Several compounds showed better in vitro cytotoxicity and selectivity against MCF-7 cells than daunomycin and doxorubicin, two known DNA binding agents that are clinically-used anti-cancer agents. Although the selectivity for HT 29 and HepG2/C3A cells is generally lower, the IC_{50} values of some analogs against these two cancer cell lines were of the same magnitude as doxorubicin. Because there was no correlation between DNA binding affinity and cytotoxicity, and because topoisomerase (Topo) inhibition is another biological mechanism of action of most anthracycline drugs, Topo I/II inhibition assays with **1**–**12** were performed. Some of the compounds showed strong inhibition against these enzymes at 100 μM, but there was no clear correlation between cytotoxicity and Topo I/II inhibition ability. Topo I/II inhibition mode assays were also performed, which verified that these compounds are topoisomerase suppressors, not poisons. Based on these results, we conclude that although DNA binding and/or topoisomerase inhibition may contribute to the observed cytotoxicity of **1**–**12**, other mechanisms of action are also likely to be important.

1. Introduction

In the 1960s, daunorubicin (Dauno) and doxorubicin (Dox), two of the most important members of the anthracycline antibiotic family (Chart 1), were isolated from two different strains of *Streptomyces pencetius*.[1,2] The subsequent discovery of their pharmaceutical potential has led to the identification of other semi-synthetic anthracyclines such as idarubicin,[3] valrubicin,[4] epirubicin,[5] pirarubicin,[6] and aclarubicin.[7,8] To date, these anthracycline antibiotics are used as frontline treatments for a variety of tumors, either alone or in combination with other drugs.[9] However, two major problems limit their clinical use: rapidly-developed drug resistance[10] and irreversible cardiac toxicity.[11,12]

All of the clinically-used anthracycline antibiotics described above share a common structure: an anthraquinone-containing tetracyclic domain connected to a carbohydrate domain via an α-glycosidic linkage. The presence of the anthraquinone core in these molecules poses a dilemma to designing new analogs with better pharmaceutical efficacy.[13] On one hand, the anthraquinone moiety is required for DNA intercalation, which is a fundamental functional mechanism for the anti-cancer activity of anthracyclines in the typical range of steady-state plasma drug concentrations.[11]

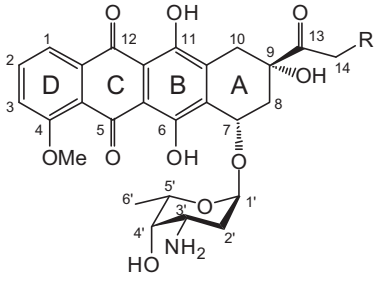

Daunorubicin: R = H
Doxorubicin: R = OH

Chart 1. Structures of daunorubicin (Dauno) and doxorubicin (Dox). The anthraquinone domain is composed of rings B, C, and D.

On the other hand, the single-electron reduction of the anthraquinone C ring leads to the generation of oxygen free radicals and related reactive oxygen species, which causes long-term toxicity to healthy cardiac tissues.[13,14]

Based on the crystal structure of the daunomycin–DNA complex, it has been established that most anthracycline antibiotics bind to DNA through intercalation of the anthraquinone moiety

* Corresponding author. Tel.: +1 780 492 1861; fax: +1 780 492 7705.
E-mail address: tlowary@ualberta.ca (T.L. Lowary).

0968-0896/$ - see front matter © 2010 Elsevier Ltd. All rights reserved.
doi:10.1016/j.bmc.2010.10.054

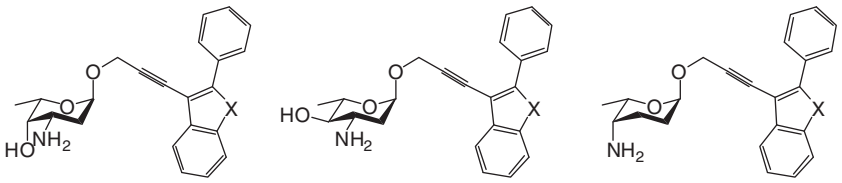

1 X = O
2 X = S
3 X = NTs
4 X = NH

5 X = O
6 X = S
7 X = NTs
8 X = NH

9 X = O
10 X = S
11 X = NTs
12 X = NH

Chart 2. Structures **1**–**12**.

between adjacent nucleoside base pairs, while the carbohydrate residue binds in the minor groove.[15,16] Using a molecular hybridization approach,[17,18] we recently reported the synthesis of a novel class of molecules designed to be functional mimics of the anthracyclines, **1**–**12** (Chart 2).[19] In these compounds, the anthraquinone moiety was replaced with one of three simple planar aromatic systems, which was linked to the minor groove binding carbohydrate moiety with a propargyl linker. We hoped that the removal of the anthraquinone moiety would avoid cardiac toxicity while at the same time, the desired cytotoxicity could be maintained through potential 'minimal' DNA binding (intercalation).[20,21]

The binding of **1**–**12** to DNA, albeit with rather weak affinity, has been confirmed using fluorescence measurements.[19] Subsequent investigations demonstrated that some of these compounds exhibit anti-bacterial activity in vitro against *Bacillus atrophaeus*, ATCC 9372 at concentrations only 2–4-fold higher than Dauno and Dox.[22] Moreover, for most of the compounds, a correlation between DNA binding affinity and anti-bacterial activity was observed, suggesting that the biological activity may be the result of DNA binding. With sufficient quantities of **1**–**12** in hand after optimization of the synthetic routes,[22] we report here the evaluation of their cytotoxicity to both tumor and non-tumor mammalian cell lines. After validating their cytotoxicity, we further explored possible functional mechanisms of this class of molecules.

2. Results and discussion

2.1. Cytotoxicity

2.1.1. In vitro cytotoxicity of 1–12 against cancer cell lines

We first evaluated the cytotoxicity of **1**–**12** against three solid-tumor cancer cell lines—MCF-7 breast cancer, HT-29 colon cancer, and HepG2/C3A liver cancer—using the 5-(3-carboxymethoxyphenyl)-2-(4,5-dimethylthiazolyl)-3-(4-sulfophenyl)tetrazolium, inner salt (MTS) cell viability assay.[23] Cytotoxicity data for **1**–**12** along with those obtained for Dauno and Dox are presented in Table 1. In addition to target compounds **1**–**12**, fragments synthesized as controls (**13**–**27**, Chart 3) were also tested. The results of this screening are summarized in Table S1 (Supplementary data). The cytotoxicity profile against these three cell lines allowed us to draw conclusions about the effect of each of the three structural components of these molecules—the aromatic domain, the linker, and the carbohydrate—on cytotoxicity.

Compounds **13**–**16**, which contain only the aromatic groups with iodine at C-3, showed no or very little cytotoxicity against all three cancer cell lines. When iodine was replaced with hydrogen, the resulting compounds, **17**–**20**, demonstrated, for the most part, little improvement in cytotoxicity. Although **19** has low cytotoxicity against MCF-7 cells, it was active against HepG2/C3A cells,

Table 1
Cytotoxicity of **1**–**12**, Dauno, and Dox against three solid-tumor cell lines[a,b,c]

Compd	Cell viability (%) at 25 μM			IC_{50} (μM)		
	MCF7	HT29	HepG2[d]	MCF7	HT29	HepG2
Dauno	2 (0.6)[e,g]	11 (2.1)[e,g]	2 (0.7)[f,g]	5.5 ± 0.5[h]	0.4 ± 0.1[f]	0.7 ± 0.2
Dox	47 (3.3)[e,g]	43 (5.0)[e,g]	8 (1.3)[f,g]	16.8 ± 1.9[h]	0.6 ± 0.1[f]	1.0 ± 0.2
1	<1	<1	<1	6.6 ± 2.0	5.2 ± 1.5	3.2 ± 0.3
2	<1	<1	<1	7.1 ± 1.2	2.6 ± 0.5	6.0 ± 1.4
3	<1	<1	<1	4.8 ± 1.1	6.3 ± 1.2	5.9 ± 1.2
4	<1	<1	<1	15.9 ± 2.0	14.0 ± 1.8	12.9 ± 1.7
5	<1	<1	<1	5.4 ± 0.7	6.5 ± 1.7	7.7 ± 1.2
6	2 (0.3)	<1	2 (0.6)	15.8 ± 3.2	10.9 ± 1.3	17.2 ± 2.6
7	<1	<1	<1	4.7 ± 1.0	7.3 ± 1.4	7.7 ± 2.0
8	2 (0.3)	7 (1.0)	<1	17.3 ± 2.3	19.3 ± 3.1	16.2 ± 1.9
9	<1	<1	<1	10.3 ± 0.2	6.5 ± 1.8	7.9 ± 0.7
10	<1	<1	<1	7.1 ± 1.2	5.9 ± 0.5	8.8 ± 0.9
11	<1	<1	<1	5.1 ± 0.4	5.4 ± 0.2	9.5 ± 0.5
12	<1	<1	<1	10.8 ± 1.8	9.2 ± 1.0	11.4 ± 2.0

[a] MTS assay, 3 days exposure to compounds.
[b] The purity of each compound is greater than 98% based on HPLC.[15]
[c] The numbers in parenthesis represent the standard deviation. All standard deviations are calculated from three independent experiments.
[d] HepG2/C3A is simplified as HepG2.
[e] At 20 μM.
[f] At 16 μM.
[g] See Figure S1 for details (Supplementary data).
[h] Unlike other compounds and other cell lines, Dauno and Dox had only a cytostatic, rather than a cytotoxic, effect on MCF-7 cells under these assay conditions.

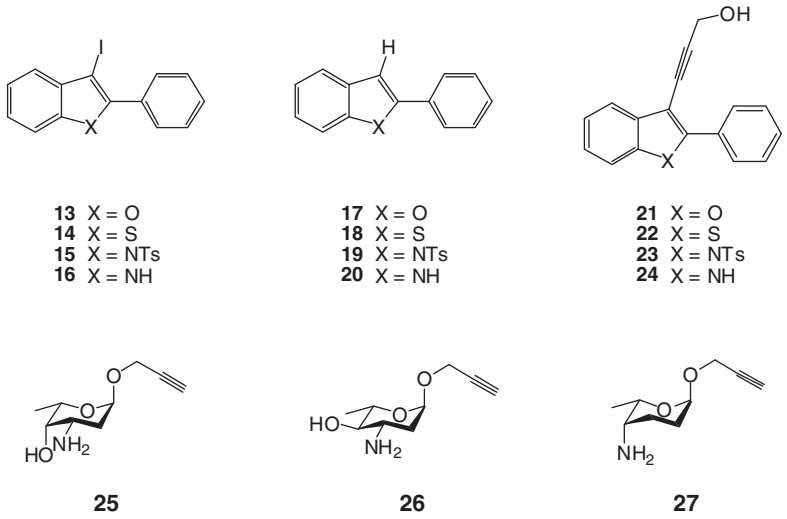

Chart 3. Fragment structures tested in the cytotoxicity assay.

with even more potency against HT-29. At 100 μM, cell viability for HT-29 decreased from 82% for compound **15** to 12% for compound **19**. When tested at 25 μM, compound **19** showed 61% cell death.

Next, the effect of the introducing a propargyl group to the C-3 position of the aromatic ring was studied. The incorporation of the propargyl linker into compound **19** (*N*-tosyl indole **23**) resulted in a very small effect on cytotoxicity. Given this result, it was unexpected that compounds **21** and **22**, derived from incorporation of the propargyl linker into either benzofuran or benzothiophene derivatives, had enhanced cytotoxicity. For example, compound **21** showed almost 100% cell death at 100 μM. However, both **21** and **22** had almost no, or very weak, activity at 25 μM.

Finally, we studied the effect of adding the carbohydrate domain. When daunosamine, acosamine, or 4-amino-2,3,4,6-tetradeoxy-α-L-*threo*-hexopyranosyl (4-*N*-TDTH) was incorporated into compounds **21**–**24**, leading to **1**–**12**, potent cytotoxicity was recovered (~100% cell death at 25 μM, Table 1). Although the introduction of the carbohydrate enhanced the cytotoxic activity of the aromatic systems, the removal of the intercalators from **1** to **12**, which afforded glycosides **25**–**27**, caused complete loss of cytotoxicity (Table S1 in Supplementary data). Two conclusions can be drawn from these observations. First, the aromatic moiety is a key component for biological activity. Second, the presence of the carbohydrate and the propargyl linker significantly enhances the cytotoxicity.

Having established the relative potency of the compounds, IC_{50} values were determined (Table 1, Fig. S1 in Supplementary data). To decrease the number of cytotoxicity assays to be carried out, these values were determined only for the compounds that, when tested at 25 μM, resulted in cell viability of less than 20%. From these IC_{50} values, it is clear that compared to the anthracycline natural products Dauno and Dox, all of the synthetic compounds are less cytotoxic against both HT-29 colon cancer cells and HepG2/C3A liver cancer cells. For MCF-7 breast cancer cells, however, the IC_{50} values of compounds **3**, **5**, **7**, and **11** (4.8, 5.4, 4.7, and 5.1 μM, respectively) were comparable to that of Dauno (5.5 μM). Compared to the IC_{50} value of Dox (16.8 μM), the cytotoxicity of most of the compounds were 2–4-fold greater, with only **4**, **6**, and **8** being less potent.

Some trends emerge from these data. In general, cytotoxicity appears to be closely correlated with the heteroatoms in the aromatic domain. Overall, enhanced cytotoxicity was observed when the aromatic groups contained either oxygen or the *N*-tosyl group (compounds **1**, **3**, **5**, **7**, **9**, and **11**). On the other hand, when this moiety contained an unprotected nitrogen (compounds **4**, **8**, and **12**), the cytotoxicity decreased significantly. For the sulfur-containing aromatic moiety, the cytotoxicity was influenced by the attached carbohydrate with a ranking of daunosamine (**2**) > 4-*N*-TDTH (**10**) > acosamine (**6**), especially against HT 29 and HepG2/C3A cell lines. At this point, we are unsure if this trend for the carbohydrate moiety implies that the stereochemistry at C-4 is a key structural feature for the cytotoxicity. Regardless, compared to the aromatic moieties, the carbohydrate moieties generally had less influence on cytotoxicity, although daunosamine appeared to be preferred.

2.1.2. In vitro cytotoxicity of active analogs against non-tumor cell lines

Having established that some of the analogs showed relatively good in vitro cytotoxicity against these three cancer cell lines, it was of interest to know if they are also toxic to normal cells. Although normal human cells are considered more suitable for toxicity evaluation,[24] normal cells from non-human sources are also extensively used to assess the specificity of cytotoxic compounds.[25,26] Therefore, human normal skin cells (ATCC CRL-7761), together with monkey kidney (Vero) and mouse lung (NIH/3T 3) cells, were employed to evaluate the toxicity of compounds with an IC_{50} value below 10 μM against any of three cancer cell lines (Table 2).

Table 2
Cytotoxicity of Dauno, Dox, and active analogs among **1**–**12** against three non-tumor cell lines[a,b,c]

Compd	IC_{50} (μM)		
	CRL-7761	Vero	NIH/3T3
Dauno	10.5 ± 1.4	2.5 ± 0.7	1.8 ± 0.3
Dox	>25	10.4 ± 1.0	3.5 ± 0.8
1	16.7 ± 2.0	5.7 ± 0.9	4.8 ± 1.1
2	22.2 ± 1.9	9.4 ± 0.6	5.7 ± 0.5
3	16.5 ± 2.1	10.2 ± 1.3	5.0 ± 0.5
5	>25	10.6 ± 1.7	6.5 ± 1.2
7	24.3 ± 2.9	11.6 ± 2.0	5.8 ± 1.0
9	>25	10.9 ± 1.6	3.7 ± 0.4
10	>25	18.1 ± 2.2	9.8 ± 1.3
11	17.5 ± 1.4	10.1 ± 1.3	4.9 ± 0.6
12	24.0 ± 2.1	20.5 ± 1.5	14.7 ± 1.9

[a] MTS assay, 3 days exposure to compounds.
[b] The purity of each compound is greater than 98% based on HPLC.[15]
[c] The numbers in parenthesis represent the standard deviation. All standard deviations are calculated from three independent experiments.

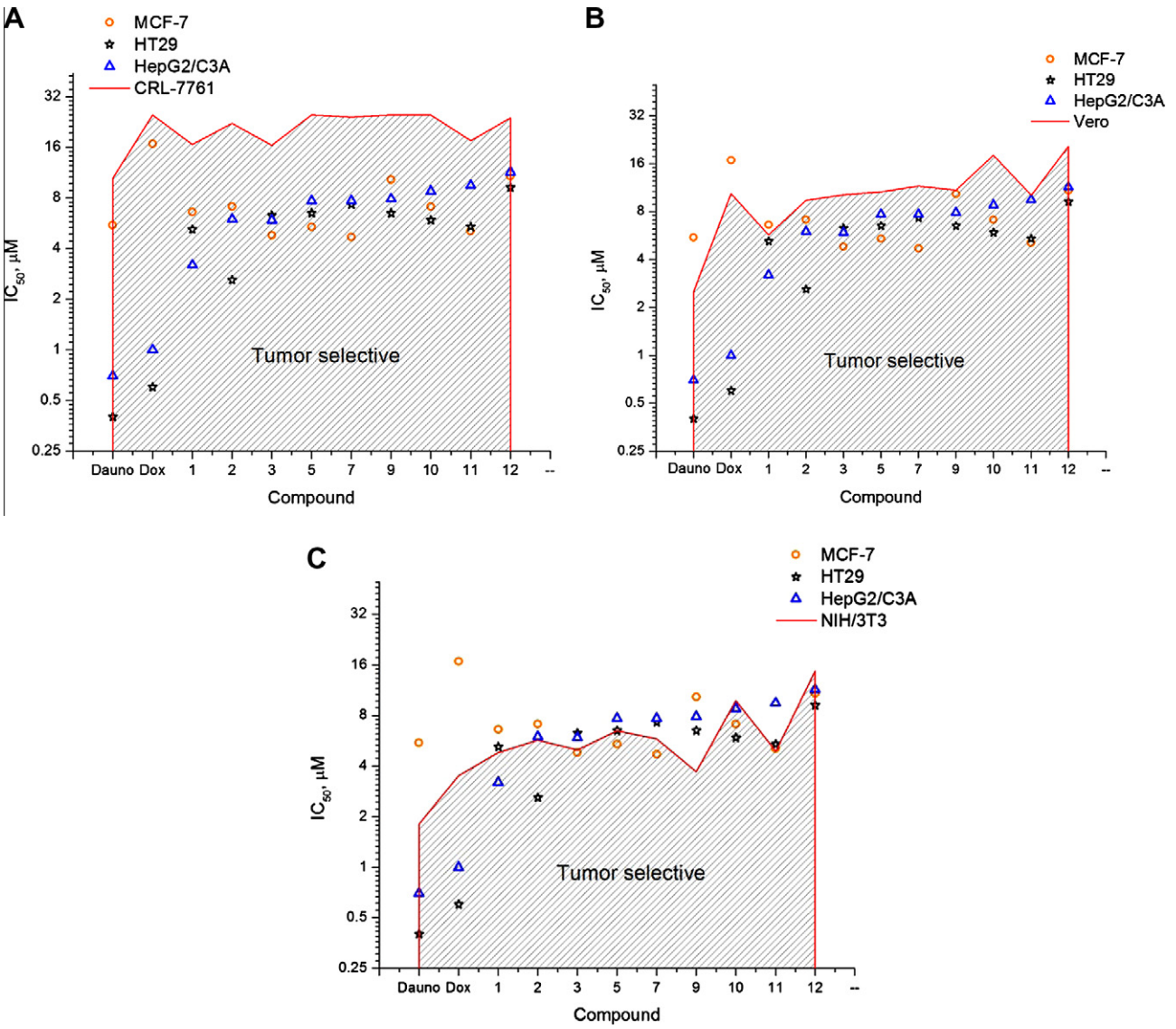

Figure 1. Cancer cell selectivity of Dauno, Dox, and active analogs among **1**–**12** against CRL-7761 human normal skin cells (**A**), Vero monkey kidney cells (**B**), and NIH/3T3 mouse lung cells (**C**). Cells (6000) were incubated with a solution of each tested compound for 72 h. MTS dye was added, and cells were incubated for another 2–3 h before the absorbance was recorded at 490 nm. The *y*-axis is logarithmic in each diagram. The top boundary of the shadowed area represents the IC_{50} value of that compound for the reference non-tumor cell line. To simplify the figure, the error bars are not shown.

The IC_{50} values obtained for the non-tumor cells can be used as a standard against which to determine the drug selectivity between normal cells and cancer cells under in vitro assay conditions. The three non-tumor cell lines provided three standards (Fig. 1). In each diagram, the shadowed area is the cancer cell selective area. The top boundary is constructed with the IC_{50} values against the non-tumor cell line used as the standard. The further below the top boundary an IC_{50} is the better selectivity this compound has between normal and cancer lines.

In Figure 1A, which compares the cytotoxicity of **1**–**12** with the CRL-7761 cell line, all compounds show cancer cell selectivity. Compared to Dauno and Dox, active analogs showed better selectivity between CRL-7761 and MCF-7 cells. In Figure 1B, when the comparison is against Vero cells, Dauno, Dox, and compound **1** are not selective for MCF-7 breast cancer cells. In addition, cancer cell selectivity decreases for all compounds, including Dauno and Dox, as all the IC_{50} values are closer to the top boundary. Furthermore, in Figure 1C, only a few of analogs exhibit cancer cell selectivity when compared against NIH/3T 3 cells. The most pronounced are **2** and **10** for HT 29 colon cancer cells, and **1** for HepG2/C3A liver cancer cells. Compared to Dauno and Dox, however, the selectivity of these compounds towards HT 29 and HepG2/C3A is much smaller.

2.1.3. Correlation of cytotoxicity with DNA binding affinity

Even though we have demonstrated that **1**–**12** are capable of binding to DNA, to confirm if DNA binding is the major mechanism leading to cell death, we correlated the cytotoxicity of **1**–**12** with DNA binding affinity (Fig. 2). The red solid line represents DNA binding affinity as the percentage of remaining EtBr in a fluorescent intercalator displacement (FID) assay.[19] The dashed lines with different symbols are constructed based on the IC_{50} values of **1**–**12**. By looking at the trends of the three dashed curves, it can be concluded that the cytotoxicity trends for all three cancer lines are very similar. Compared to the DNA binding affinity curve, the 12 compounds can be divided into three groups. In the first group, (**10**, **12**, **4**, and **8**), the cytotoxicity trend is inversely related to the DNA binding of the molecule. In the second group, (**6**, **9**, **2**, and possibly **8** and **1**), the cytotoxicity trend matches the overall

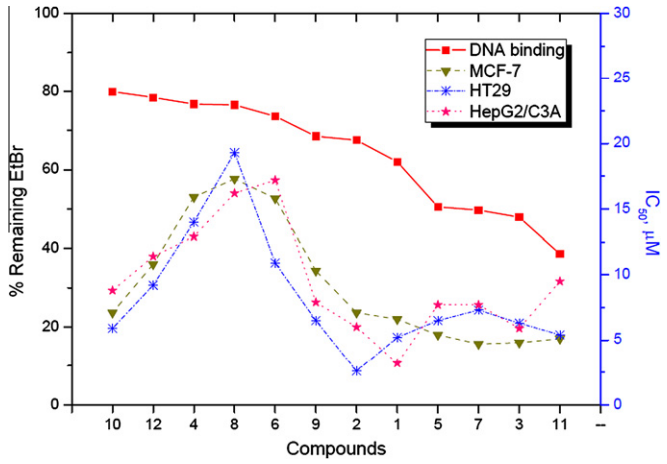

Figure 2. Correlation between cytotoxicity and DNA binding affinity.

DNA binding trend, but the amplitude of the changes is quite different. In the last group consisting of **1**, **5**, **7**, **3**, and **11**, which are the most cytotoxic among the analogs, there is no clear correlation between cytotoxicity and DNA binding. Taken together, the above analysis suggests that DNA binding is not the primary mode of action of most, if not all, of these compounds.

2.2. Topoisomerase inhibition

In the typical range of steady-state plasma drug concentrations (<1 μM), in addition to DNA binding, the other well-accepted functional mechanism for the anthracycline antibiotics is topoisomerase inhibition by stabilizing the complex of topoisomerase and cleaved DNA.[27] Because compared to Dauno and Dox, some anthracycline analogs with greatly reduced DNA binding affinity still show similar capacity to inhibit topoisomerase II (Topo II),[28,29] we thought that it would be worthwhile to investigate the Topo II inhibition ability of **1**–**12**. Although Topo II is the main target enzyme of the anthracycline antibiotics,[13] it has been reported that some also inhibit topoisomerase I (Topo I).[30] Therefore, **1**–**12** were also screened against Topo I.

2.2.1. Inhibition of topoisomerase I

A standard plasmid cleavage assay was used to investigate the effect of Dauno, Dox and **1**–**12** on recombinant human Topo I by DNA gel electrophoresis under cell-free conditions.[31,32] This assay provides a direct means of determining if the drug affects the unwinding of a supercoiled (SC) duplex DNA substrate, because the enzyme converts SC DNA to relaxed (R) DNA and nicked open circular (NOC) DNA. NOC DNA is double stranded DNA with a cleaved strand, which is formed because the enzyme cleaves only one DNA strand at a time. SC DNA migrates fastest on an agarose gel, the NOC DNA slowest and R DNA in middle (Figure 3). If Topo I retains its normal activity, one would expect to see the disappearance of SC DNA (fastest band) and the appearance of bands for R DNA and NOC DNA. On the contrary, if the activity of the enzyme is inhibited, no R DNA or NOC DNA would be detected.

Initially, all compounds were tested at 100 μM. From the gels shown in Figure 3A, compounds **4** (lane 8), **8** (lane 12), **10** (lane 14), and **12** (lane 16) showed very light bands for SC DNA and a series of bands for R DNA, indicating their weak inhibition of Topo I. Compared to the R DNA marker (lane 1), a series of bands corresponding to partially relaxed DNA could be seen for compounds **2** (lane 6), **5** (lane 9), **6** (lane 10), and **9** (lane 13) indicating that these four compounds had a partial inhibitory effect on Topo I. In contrast, the almost equal intensity of the SC DNA and R DNA bands in lane 15 indicates that **11** showed moderate Topo I inhibition. On the other hand, strong SC DNA bands and very light R DNA bands can be seen for compounds **1** (lane 5), **3** (lane 7), and **7** (lane 11). Thus **1**, **3**, and **7** all significantly inhibit Topo I catalysis when tested at a 100 μM concentration. However, when the concentration was decreased to 40 μM and below, all compounds showed much weaker Topo I inhibition compared to 5 μM of Dauno (lane 22) and Dox (lane 23) (Figure 3C).

Because DNA binding is one of the modes for topoisomerase inhibition,[13] it is of interest to determine if there is any correlation between these two properties for **1**–**12**. Topo I inhibition ratios compared to the DMSO control were quantitated (Fig. 3C and D) and the data at 100 μM are listed in Table 3. It appears that DNA binding benefits Topo I inhibition (compounds **3** and **7**), but not always (compounds **1** and **11**). Another interesting finding is that although **2** (lane 6) **5** (lane 9), **6** (lane 10), **9** (lane 13), and **11** (lane 15) all showed partial Topo I inhibition, the pattern of DNA bands for **11** is very distinct from that for the others; no partially relaxed DNA bands could be seen. This is presumably because of the relatively strong DNA binding affinity of **11**, which prevents the enzyme from efficiently binding to the DNA. However, confirmation of this requires additional study.

2.2.2. Inhibition of topoisomerase II

We also examined the ability of **1**–**12** to inhibit the activity of human topoisomerase II-catalyzed decatenation of kDNA.[33] The decatenation reaction is specific to Topo II as it involves the simultaneous cleavage of two DNA strands of a double-stranded DNA helix.[31,32] The reaction was followed by gel electrophoresis, monitoring the appearance of kDNA monomers in the form of either nicked, open circular decatenated (NOC) kDNA or closed circular decatenated (CC) kDNA. The NOC kDNA is formed by the action of Topo II on the nicked kDNA substrate, which is generated during the isolation of kDNA.[34] On the gel, catenated (C) kDNA has the lowest mobility, CC kDNA migrates the furthest, whereas NOC kDNA has intermediate mobility (Fig. 4). Using this assay, Dauno, Dox, and **1**–**12** were tested for their ability to inhibit the enzyme. If Topo II retains its normal function, the C kDNA (top band) would disappear and bands for both NOC kDNA and CC kDNA would appear. On the contrary, the absence of NOC DNA and CC DNA bands indicates inhibition of the enzyme.

As shown in Figure 4, no obvious inhibitory effects were observed for compounds **1** (lane 4), **2** (lane 5), **4** (lane 8), **5** (lane 10), **6** (lane 11), **8** (lane 13), **9** (lane 14), **10** (lane 15), and **12** (lane 17) at a concentration of 100 μM. However, compounds **3** (lanes 6 and 7), **7** (lane 12), and **11** (lane 16) showed almost complete inhibition of topoisomerase II at the same or even lower concentration. As noted above, compounds **3** and **7** also showed strong topoisomerase I inhibition. Some of these compounds were tested at lower concentrations, for example, 40 μM and 20 μM (Fig. S2 in Supplementary data). At 40 μM, only compounds **3**, **7**, **11** still exhibited a moderate inhibitory effect. All these compounds contain a large tosyl group in the aromatic core and the effect of this group on the inhibition of both enzymes requires further exploration. None of these three compounds inhibited the enzyme at 20 μM. As observed for Topo I, compared to Dox and Dauno (Fig. S2), these compounds showed weaker Topo II inhibition ability.

Quantitation of Topo II inhibition was also analyzed (Fig. 4B) and listed in Table 3. Similar to the observations with Topo I, for **1**–**12** there is some correlation between DNA binding affinity and Topo II inhibition at the concentration of 100 μM (Table 3). We note that **1** showed selective inhibition against Topo I, whereas **8** and **12** have some selectivity against Topo II.

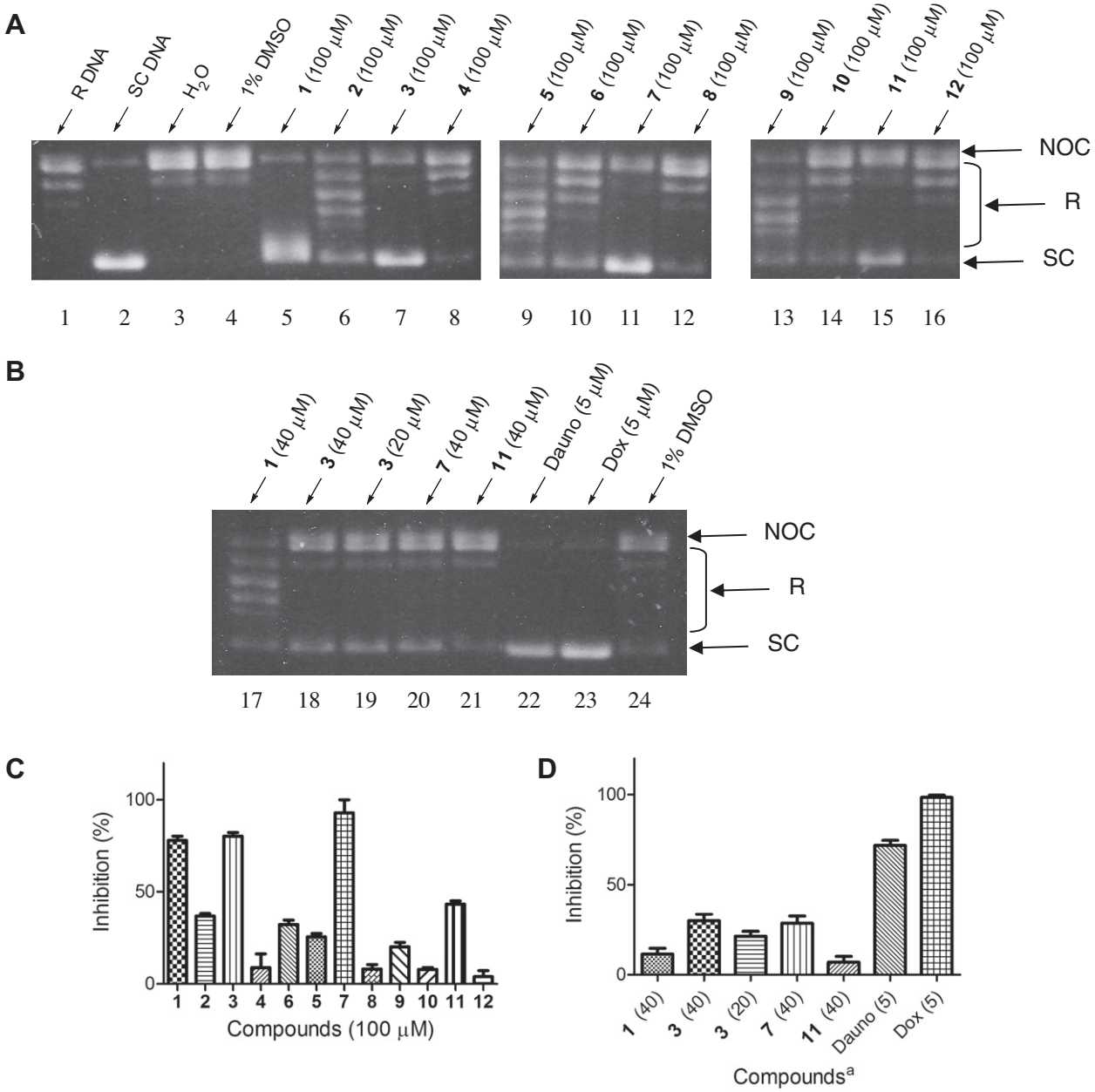

Figure 3. Topo I Inhibition assays. (A) Gel images for Topo I inhibition of **1**–**12** at 100 μM; (B) gel images for Topo I inhibition of Dauno (5 μM), Dox (5 μM), and **1**–**12** (20 or 40 μM); (C) DMSO-normalized inhibition ratios of **1**–**12** at 100 μM; (D) DMSO-normalized inhibition ratios of Dauno (5 μM), Dox (5 μM), and **1**–**12** (20 or 40 μM). Supercoiled DNA (0.25 μg) and 1.25 units of Topo I were incubated for 45 min in the presence or absence of various compounds. Quantitative inhibition was calculated based on the formula $[1 - SC_s/SC_c] \times 100\%$, where SC_s stands for the intensity of the SC DNA band for a sample and SC_c for the intensity of the SC DNA band for the DMSO control. [a]The number in parenthesis is the concentration in μM at which the compound was assayed.

2.2.3. Studies on topoisomerase inhibition mode

After some analogs were confirmed to inhibit both Topo I and II, we determined the mode of inhibition. Topoisomerase inhibitors can be classified as either poisons or suppressors based on the manner in which they interfere with the action of these enzymes.[35,36] Poisons stabilize the cleavable enzyme–DNA complex; suppressors prevent the formation of such a complex. By detecting the presence or absence of the cleavable complex, poisons can therefore be distinguished from suppressors.

Circular supercoiled plasmid (SC) DNA is used as the substrate in the inhibition mode assay. If a compound is a topoisomerase suppressor, the DNA starting material will remain intact because the topoisomerase catalyzed cleavage of DNA is blocked by the suppressor. If a compound is a topoisomerase poison, DNA cleavage will occur in the presence of the enzyme. Subsequently, the cleaved DNA product will be stabilized by poisons through the formation of a cleavable enzyme–inhibitor–DNA complex. Thereafter, the cleaved DNA products, nicked open circular (NOC) DNA for Topo I and linear (L) DNA for Topo II, can be trapped by sodium dodecyl sulfate (SDS). Subsequent proteinase K digestion removes the bound enzymes. After resolution of DNA species by gel electrophoresis, the presence or absence of the NOC DNA band will classify the inhibitor as a Topo I poison or suppressor, as will the presence or absence of the L DNA band for Topo II.

As illustrated in Figure 5, at a concentration of 100 μM, no NOC DNA or L DNA band was observed for compounds that showed Topo I or II inhibition in the previous assays, which indicates that they are topoisomerase suppressors, not poisons. In contrast,

Table 3
Correlation between DNA binding affinity and Topo inhibition ability for **1–12** (100 μM)

Compound	Rel. DNA binding (% Remaining EtBr)[a] (%)	Topo I inhibition (%)	Topo II inhibition (%)
1	62.0	77.8 ± 4.0	6.5 ± 3.3
2	67.5	36.9 ± 2.2	5.8 ± 4.0
3	47.9	80.1 ± 3.5	101 ± 6.1
4	76.7	8.8 ± 13.1	7.1 ± 4.8
5	50.5	25.5 ± 3.2	5.5 ± 3.7
6	73.6	32.2 ± 4.1	22.2 ± 3.0
7	49.7	92.8 ± 12.5	103 ± 4.4
8	76.5	8.2 ± 4.1	55.5 ± 2.7
9	68.5	20.2 ± 4.1	0 ± 0.6
10	79.9	7.9 ± 1.9	16.4 ± 3.1
11	38.6	43.2 ± 3.2	86.2 ± 3.3
12	78.4	4.0 ± 5.8	39.5 ± 3.4

[a] From Ref. 15.

NOC DNA and L DNA were clearly visible for positive control compounds, camptothecin (CPT, lane 4) for Topo I, and etoposide (VP-16, lane 11) for Topo II.

It has been reported that the strong DNA intercalation ability of some anthracyclines can suppress topoisomerase-mediated DNA cleavage, thus masking the poisoning effect of the compounds.[37] This might explain why no L DNA band was observed for Dox in lane 12 Figure 5. Although DNA binding affinity of these compounds derived from the FID assays is low compared to the anthracyclines, we nevertheless carried out a serial dilution test for Topo I inhibition by compound **3**, which showed the strong inhibition against both Topo I and II. The conclusion is the same, that no topoisomerase poisoning could be detected (Fig. S3 in Supplementary data). Although we can safely conclude that **1**, **3**, **7** and **11** are not topoisomerase poisons under our assay conditions, the mechanism by which they inhibit the enzymes is unclear.

2.2.4. Correlation of cytotoxicity with topoisomerase inhibition ability

As outlined above (Figure 2), it has been shown that DNA binding is likely not the major mode of action for this class of compounds. Because some analogs (**2** and **5**) with rather poor Topo I or II inhibition still exhibited similar cytotoxicity compared to the ones with higher potency against Topo I or II, we conclude that topoisomerase inhibition may not be the major mode of action of these compounds. Other data presented above also provides indirect support for these conclusions. Dauno and Dox show much stronger DNA binding and topoisomerase inhibition than **1–12**. Therefore, the comparable cytotoxicity of **3**, **7**, and **11** with Dauno and Dox against MCF-7 cells suggests that other pathways must be the major targets for these compounds. However, because most of the compounds with relatively strong DNA binding affinity and/or topoisomerase inhibition ability were also more cytotoxic, we cannot exclude the possibility that in the complex physiological network, these two cellular targets are partially involved in the functional mechanisms of action.

3. Conclusions

In summary, in vitro cell viability assays were employed to investigate the inhibition effect of **1–12** on the growth of mammalian cells. It was found that some analogs achieved promising cytotoxicity with IC_{50} values lower than 5 μM against some cancer cell lines. Of particular note is the MCF-7 breast cancer cell line, against which some of the compounds showed similar toxicity to Dauno and better cytotoxicity than Dox. Subsequently, active analogs were screened against three non-tumor cell lines. Under the assay conditions, all of the compounds showed better MCF-7 cancer cell selectivity than Dauno and Dox. Some analogs also exhibited HT 29 colon or HepG2/C3A liver cancer cell selectivity, although they are not as selective as Dauno and Dox.

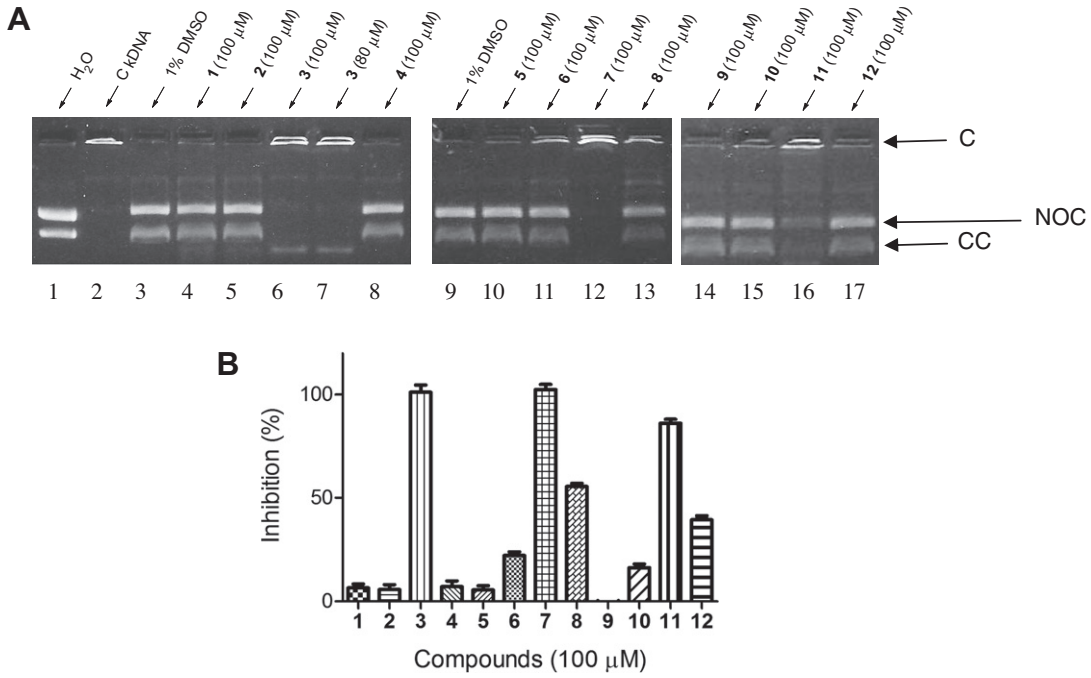

Figure 4. Topo II inhibition assays. (A) Gel images for Topo II Inhibition of **1–12** at 80 or 100 μM; (B) DMSO-normalized inhibition ratios of **1–12** at 100 μM. Kinetoplast DNA (0.17 μg) and one unit of Topo II were incubated for 30 min in the presence or absence of various compounds. Quantitative inhibition was calculated based on the formula $[1 - (NOC + CC)_s/(NOC + CC)_c)] \times 100\%$, where $(NOC + CC)_s$ stands for the combined intensity of both NOC and CC DNA band for a sample and $(NOC + CC)_c$ for the combined intensity of both NOC and CC DNA band for the DMSO control.

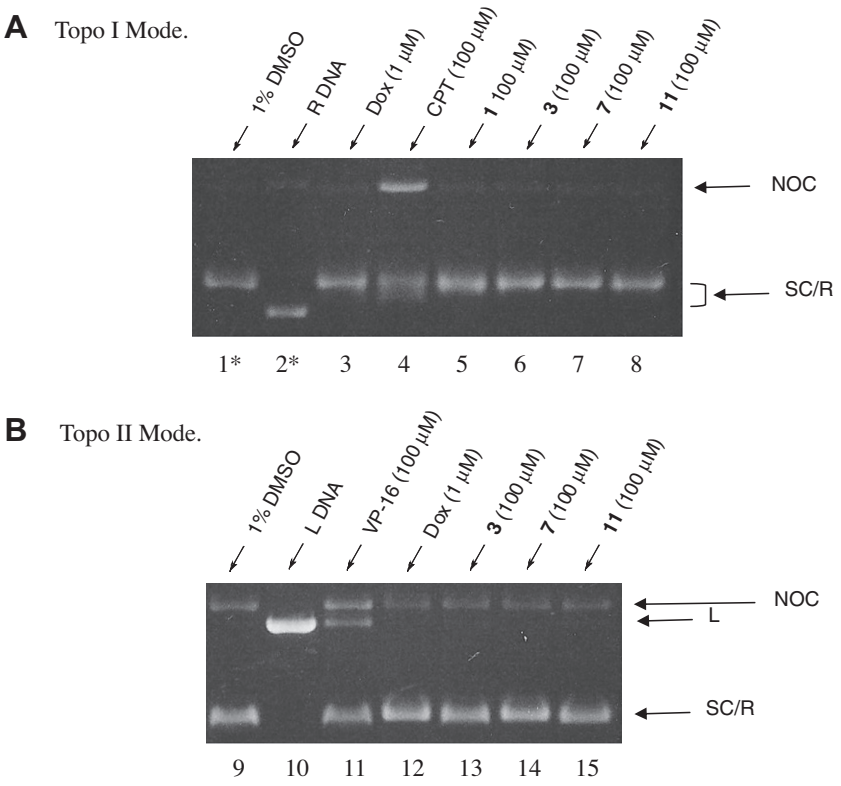

Figure 5. Topo I and Topo II Inhibition mode assay. Supercoiled DNA (0.25 μg) and six units of Topo I or four units of Topo II were incubated for 30 min in the presence or absence of various compounds. *By running the gel in EtBr-free electrolyte, the complete relaxation of SC DNA was confirmed for lane 1. The difference for R DNA between lane 2 and the others may be due to the presence of DMSO that somehow affects the mobility of R DNA.

We propose that DNA binding is likely not the major mode of action for **1**–**12**, due to the lack of correlation between cytotoxicity and previously-reported DNA binding data.[19] To explore if the observed cytotoxicity was the result of topoisomerase I or II inhibition, gel-electrophoresis assays were performed with **1**–**12**. Compounds **3**, **7**, and **11**, which possess a tosylated indole core, generally showed more potent inhibition ability against both Topo I and Topo II at 100 μM than the other analogs. Inhibition mode assays demonstrated that there were no Topo I or Topo II poisoning effects for active analogs, and that the compounds therefore act as Topo I/II suppressors. The relatively weak inhibition of Topo I/II by these compounds suggests that, unlike Dauno and Dox, topoisomerase inhibition is likely not the major mode of action, either. Given that the structures of **1**–**12** are significantly different than the anthracyclines and cognizant of the fact that some minor modifications to existing anthracycline drugs (e.g., valrubicin and AD 198, Chart 4) cause a change in their biological targets,[13] it is perhaps not surprising that the compounds studied here function in a manner different from the anthracyclines. Nevertheless, it should be appreciated that the cytotoxicity of these compounds may result, in part, from DNA binding and/or topoisomerase inhibition in addition to their influence on other biological targets. Indeed, it is possible that **1**–**12** may each exert their biological effect through differential targeting of different pathways. The mechanism by which these compounds exert their cytotoxic effect remains unknown, and studies on elucidating their mode of action are on-going.

4. Experimental section

4.1. Cytotoxicity assay

CellTiter 96® aqueous one solution MTS dye, a mixture of [3-(4,5-dimethylthiazol-2-yl)-5-(3-carboxymethoxyphenyl)-2-(4-sulfophenyl)-2*H*-tetrazolium (MTS), inner salt and an electron cou-

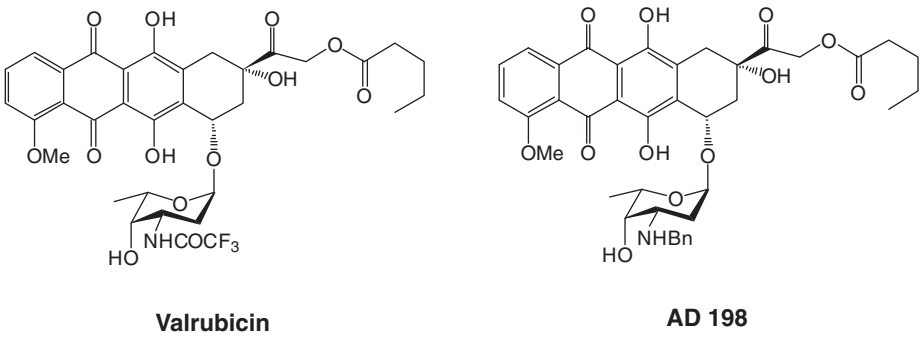

Chart 4. Structures of valrubicin and AD 198.

pling reagent (phenazine ethosulfate, PES), was obtained from Promega. DMEM high glucose culture media with sodium pyruvate, DMEM-F12 culture media, trypsin-EDTA, L-glutamine, fetal bovine serum (FBS), human transferin, bovine insulin, and phosphate-buffered saline (PBS, calcium and magnesium free), a solution of penicillin and streptomycin were purchased from Invitrogen Corp. Human albumin was purchased from Sigma. Daunomycin and Doxorubicin were obtained from IFFECT ChemPhar (Hong Kong) Company Limited.

4.1.1. Cell culture

Three cancer cell lines (MCF-7, HT-29, and HepG2/C3A) and three non-tumor cell lines (CRL-7761, Vero, and NIH/3T 3) were purchased from the American Type Culture Collection (ATCC). NIH/3T 3 mouse lung cells were maintained in DMEM/HIGH culture media supplemented with 10% calf serum, 2 mM L-glutamine, 100 unit/L penicillin, and 100 μg streptomycin. Vero monkey kidney cells were maintained in DMEM/HIGH culture media supplemented with 5% FBS, 2 mM L-glutamine, 10 mM HEPES (*N*-2-hydroxyethylpiperazine-*N*′-2-ethane sulfonic acid), 100 unit penicillin, and 100 μg streptomycin. All the rest four cell lines were maintained in DMEM/HIGH culture media supplemented with 10% FBS and 2 mM L-glutamine. Cell cultures were grown in monolayers in a humidified atmosphere of 5% CO_2 and 95% air at 37 °C. The culture media were changed every 2–3 days. Cell cultures were passaged once a week using trypsin-EDTA (0.25%) to detach the cells from their culture flasks.

4.1.2. MTS non-radioactive cell proliferation assay

Rapidly growing cells were counted and seeded at a concentration of 1×10^4 cells/well in 100 μL total volume per well into a 96-well microtiter plate. After incubation at 37 °C for 24 h, the culture medium was removed and the cell assay media (DMEM–F12 media with 1.0 mg/mL human albumin, 5.0 mg/L human transferin, and 5.0 mg/L bovine insulin) with or without tested compounds in 100 μL total volume were added to each well containing the exponentially growing cancer cells. Culture wells (triplicate to quintuplicate per sample) were incubated for three days at 37 °C (5% CO_2, 95% air). Then 20 μL of MTS dye solution was added to each sample well. After 2–2.5 h of incubation at 37 °C, the absorbance of formazan was recorded at 490 nm with a SPECTRAmax absorbance microtitre plate reader. Cell viability was calculated as a percentage of control wells, which contained the cell assay media only. Statistical and graphical analysis information was determined using Origin Pro 7.5 software (OriginLab Corp.) and Microsoft Excel (Microsoft Corp.). The determination of IC_{50} values was performed using nonlinear regression analysis based on the Boltzman function as follows:

$$y = A_2 \times \frac{A_1 - A_2}{1 + e^{(x - x_0)/\mathrm{dx}}}$$

4.2. DNA gel electrophoresis assay of topoisomerases

Recombinant human topoisomerase I (wild type protein), purified human DNA topoisomerase IIα (p170 form), supercoiled plasmid substrate DNA, kinetoplast DNA (kDNA), supercoiled pRYG DNA, camptothecin, and etoposide were purchased from Topogen Inc. Proteinase K and phenol solution were purchased from Sigma. Topoisomerase I and II assays were all performed according to protocols provided by TopoGen, Inc. All experiments were done in at least duplicate to confirm the results.

4.2.1. Inhibition assay of topoisomerase I

Reactions contained 0.25 μg supercoiled (form I) substrate DNA, assay buffer (10 mM Tris–HCl, 1 mM EDTA, 150 mM NaCl, 0.1% Bovine Serum Albumin, 0.1 mM spermidine, 5% glycerol), 1.25 units of human topoisomerase I, and the test compounds in a 20 μL final volume. These reaction mixtures were incubated at 37 °C for 45 min and terminated with stop loading buffer. The enzyme was then digested with proteinase K (50 μg/mL) for 30 min. Extractions were performed for the reactions containing Dauno and Dox by using the 1:1 mixture of buffer-equilibrated phenol solution and CIA ($CHCl_3$–isoamyl alcohol, 24:1), but no ethanol precipitation of the DNA was necessary. CIA extractions were then performed for all the compounds, including Dauno and Dox. The blue aqueous phases containing the DNA were then loaded onto a 1% ethidium bromide-free agarose gel. The gel was run in TAE buffer at 2 V/cm until the blue band migrated across the gel. Following electrophoresis, the gel was stained in 0.5 μg/mL ethidium bromide and photographed under UV light. Using ImageJ 1.43u software, quantitative inhibition was calculated based on the formula $[1 - SC_s/SC_c] \times 100\%$, where SC_s stands for the intensity of the SC DNA band for a sample and SC_c for the intensity of the SC DNA band for the DMSO control. Statistical and graphical analysis information was determined using GraphPad Prism 5.00 software (GraphPad Software, Inc.).

4.2.2. Inhibition assay of topoisomerase II

Reactions contained 0.17 μg kinetoplast DNA (kDNA), the assay buffer (50 mM Tris–HCl, 5 mM ATP, 150 mM NaCl, 30 μg/mL Bovine Serum Albumin, 0.5 mM dithiothreitol, 10 mM $MgCl_2$), 1 unit of human topoisomerase IIα (p170 form), and the test compounds in a 20 μL final volume. These reaction mixtures were incubated at 37 °C for 30 min and terminated with 4 μL of stop loading buffer. After the enzyme digestion with proteinase K (50 μg/mL) for 20 min, the blue solutions containing the DNA were directly loaded onto a 1% agarose gel containing ethidium bromide (0.5 μg/mL). The products were resolved by gel electrophoresis in TAE buffer for 30 min at 100 V, which separated the catenated kDNA from the decatenated DNA monomers. The gel was then destained in water for 30 min followed by photography. Using ImageJ 1.43u software, quantitative inhibition was calculated based on the formula $[1 - (NOC + CC)_s/(NOC + CC)_c)] \times 100\%$, where $(NOC + CC)_s$ stands for the combined intensity of both NOC and CC DNA band for a sample and $(NOC + CC)_c$ for the combined intensity of both NOC and CC DNA band for the DMSO control. Statistical and graphical analysis information was determined using GraphPad Prism 5.00 software (GraphPad Software, Inc.).

4.2.3. Cleavage assay of topoisomerase I

The enzymatic reactions were set in the same format as for the Topo I inhibition assays except that an increased amount of the enzyme (6 units per reaction) was used. These reaction mixtures were incubated at 37 °C for 30 min and immediately terminated with 2 μL of 10% sodium dodecyl sulfate (SDS), followed by vigorous mixing. After the enzyme digestion with proteinase K (50 μg/mL) for 20 min, gel loading buffer was added to the reaction mixture. Afterwards, CIA extractions were employed to purify the DNA samples. For strong DNA intercalating agents such as Dauno and Dox, it was necessary to perform extra extractions with the 1:1 mixture of buffer-equilibrated phenol solution and CIA (chloroform–isoamyl alcohol, 24:1) before CIA extractions. After vigorous vortexing, the top blue solutions containing the DNA were split into two equal portions. One portion was loaded onto a 1% ethidium bromide-free agarose gel, and the gel was run in ethidium bromide-free TAE buffer at 2 V/cm. Following electrophoresis, the gel was stained in 0.5 μg/mL ethidium bromide and the gel visualized under UV light. The other portion was resolved on a 1% ethidium bromide-containing agarose gel in ethidium bromide-containing TAE buffer also at 2 V/cm. After destaining in water, the poisoning activity of the tested samples was determined

by the presence or absence of the nicked open circular (NOC) DNA band, which was obtained from the positive control, Camptothecin.

4.2.4. Cleavage assay of topoisomerase II

Reactions contained 0.25 μg pRYG supercoiled DNA, the assay buffer (50 mM Tris–HCl, 2 mM ATP, 30 μg/ml Bovine Serum Albumin, 0.5 mM dithiothreitol, 150 mM NaCl, 10 mM $MgCl_2$), 4 units of human topoisomerase IIα (p170 form), and the test compounds in a 20 μL final volume. After the reaction mixtures were incubated at 37 °C for 30 min, the same procedures for the Topo I cleavage assays were followed. The poisoning activity of the tested samples was determined by the presence or absence of the linear DNA band.

Acknowledgements

This work was supported by the University of Alberta, the Natural Sciences and Engineering Research Council of Canada and the Alberta Ingenuity Centre for Carbohydrate Science. W.S. is the recipient of a Studentship from the Alberta Ingenuity Fund.

Supplementary data

Table S1 (cytotoxicity of **13**–**27** against three solid-tumor cell lines), cytotoxicity curves of Dauno, Dox, and compounds **1–8** against three cancer cell lines, and two figures for Inhibition assay of Topo II (low concentrations) and inhibition mode assay of compound **3** against Topo I. Supplementary data associated with this article can be found, in the online version, at doi:10.1016/j.bmc.2010.10.054.

References and notes

1. Dimarco, A.; Gaetani, M.; Orezzi, P.; Scarpinato, B. M.; Silvestrini, R.; Soldati, M.; Dasdia, T.; Valentini, L. *Nature* **1964**, *201*, 706.
2. Arcamone, F.; Cassinelli, G.; Fantini, G.; Grein, A.; Orezzi, P.; Pol, C.; Spalla, C. *Biotechnol. Bioeng.* **1969**, *11*, 1101.
3. Arcamone, F.; Bernardi, L.; Giardino, P.; Patelli, B.; Marco, A.; Casazza, A. M.; Pratesi, G.; Reggiani, P. *Cancer Treat. Rep.* **1976**, *60*, 829.
4. Israel, M.; Modest, E. J.; Frei, E., 3rd. *Cancer Res.* **1975**, *35*, 1365.
5. Coukell, A. J.; Faulds, D. *Drugs* **1997**, *53*, 453.
6. Umezawa, H.; Takahashi, Y.; Kinoshita, M.; Naganawa, H.; Masuda, T.; Ishizuka, M.; Tatsuta, K.; Takeuchi, T. *J. Antibiot. (Tokyo)* **1979**, *32*, 1082.
7. Oki, T.; Matsuzawa, Y.; Yoshimoto, A.; Numata, K.; Kitamura, I. *J. Antibiot. (Tokyo)* **1975**, *28*, 830.
8. Hori, S.; Shirai, M.; Hirano, S.; Oki, T.; Inui, T.; Tsukagoshi, S.; Ishizuka, M.; Takeuchi, T.; Umezawa, H. *Gann.* **1977**, *68*, 685.
9. Weiss, R. B. *Semin. Oncol.* **1992**, *19*, 670.
10. Kimchi-Sarfaty, C.; Gribar, J. J.; Gottesman, M. M. *Mol. Pharmacol.* **2002**, *62*, 1.
11. Singal, P. K.; Li, T.; Kumar, D.; Danelisen, I.; Iliskovic, N. *Mol. Cell Biochem.* **2000**, *207*, 77.
12. Ng, R.; Better, N.; Green, M. D. *Semin. Oncol.* **2006**, *33*, 2.
13. Minotti, G.; Menna, P.; Salvatorelli, E.; Cairo, G.; Gianni, L. *Pharmacol. Rev.* **2004**, *56*, 185.
14. Fan, E.; Shi, W.; Lowary, T. L. *J. Org. Chem.* **2007**, *72*, 2917.
15. Qu, X.; Wan, C.; Becker, H. C.; Zhong, D.; Zewail, A. H. *Proc. Natl. Acad. Sci. U.S.A.* **2001**, *98*, 14212.
16. Wang, A. H.; Ughetto, G.; Quigley, G. J.; Rich, A. *Biochemistry* **1987**, *26*, 1152.
17. Viegas-Junior, C.; Danuello, A.; da Silva Bolzani, V.; Barreiro, E. J.; Fraga, C. A. M. *Curr. Med. Chem.* **2007**, *14*, 1829.
18. Meunier, B. *Acc. Chem. Res.* **2007**, *41*, 69.
19. Shi, W.; Coleman, R. S.; Lowary, T. L. *Org. Biomol. Chem.* **2009**, *7*, 3709.
20. Atwell, G. J.; Bos, C. D.; Baguley, B. C.; Denny, W. A. *J. Med. Chem.* **1988**, *31*, 1048.
21. Atwell, G. J.; Baguley, B. C.; Denny, W. A. *J. Med. Chem.* **1989**, *32*, 396.
22. Shi, W.; Marcus, S. L.; Lowary, T. L. *Carbohydr. Res.* **2010**, *345*, 10.
23. Barltrop, J. A.; Owen, T. C.; Cory, A. H.; Cory, J. G. *Bioorg. Med. Chem. Lett.* **1991**, *1*, 611.
24. Matsuo, M.; Sasaki, N.; Saga, K.; Kaneko, T. *Biol. Pharm. Bull.* **2005**, *28*, 253.
25. Gududuru, V.; Hurh, E.; Durgam, G. G.; Hong, S. S.; Sardar, V. M.; Xu, H.; Dalton, J. T.; Miller, D. D. *Bioorg. Med. Chem. Lett.* **2004**, *14*, 4919.
26. Petinari, L.; Kohn, L. K.; de Carvalho, J. E.; Genari, S. C. *Cell. Biol. Int.* **2004**, *28*, 531.
27. Gewirtz, D. A. *Biochem. Pharmacol.* **1999**, *57*, 727.
28. Chaires, J. B.; Dattagupta, N.; Crothers, D. M. *Biochemistry* **1985**, *24*, 260.
29. Capranico, G.; Supino, R.; Binaschi, M.; Capolongo, L.; Grandi, M.; Suarato, A.; Zunino, F. *Mol. Pharmacol.* **1994**, *45*, 908.
30. Guano, F.; Pourquier, P.; Tinelli, S.; Binaschi, M.; Bigioni, M.; Animati, F.; Manzini, S.; Zunino, F.; Kohlhagen, G.; Pommier, Y.; Capranico, G. *Mol. Pharmacol.* **1999**, *56*, 77.
31. Mizushina, Y.; Akihisa, T.; Ukiya, M.; Murakami, C.; Kuriyama, I.; Xu, X.; Yoshida, H.; Sakaguchi, K. *Cancer Sci.* **2004**, *95*, 354.
32. Montaner, B.; Castillo-Avila, W.; Martinell, M.; Ollinger, R.; Aymami, J.; Giralt, E.; Perez-Tomas, R. *Toxicol. Sci.* **2005**, *85*, 870.
33. Marini, J. C.; Miller, K. G.; Englund, P. T. *J. Biol. Chem.* **1980**, *255*, 4976.
34. Hasinoff, B. B.; Creighton, A. M.; Kozlowska, H.; Thampatty, P.; Allan, W. P.; Yalowich, J. C. *Mol. Pharmacol.* **1997**, *52*, 839.
35. Wang, J. C. *Annu. Rev. Biochem.* **1996**, *65*, 635.
36. Champoux, J. J. *Annu. Rev. Biochem.* **2001**, *70*, 369.
37. Wassermann, K.; Markovits, J.; Jaxel, C.; Capranico, G.; Kohn, K. W.; Pommier, Y. *Mol. Pharmacol.* **1990**, *38*, 38.